On the Stability of Permanent Electrochemical Doping of Quantum Dot, Fullerene, and Conductive Polymer Films in Frozen Electrolytes for Use in Semiconductor Devices

Gudjonsdottir, Solrun; Van Der Stam, Ward; Koopman, Christel; Kwakkenbos, Bob; Evers, Wiel H.; Houtepen, Arjan J.

DOI
10.1021/acsanm.9b00863

Publication date
2019

Document Version
Final published version

Published in
ACS Applied Nano Materials

ACS APPLIED NANO MATERIALS

Article

Cite This: ACS Appl. Nano Mater. 2019, 2, 4900−4909

www.acsanm.org

On the Stability of Permanent Electrochemical Doping of Quantum Dot, Fullerene, and Conductive Polymer Films in Frozen Electrolytes for Use in Semiconductor Devices

Solrun Gudjonsdottir,[†] Ward van der Stam,[†,§] Christel Koopman,[†] Bob Kwakkenbos,[†] Wiel H. Evers,[†,‡] and Arjan J. Houtepen*[,†]

[†]Chemical Engineering, Optoelectronic Materials, and [‡]Kavli Institute of Nanoscience, Delft University of Technology, Van der Maasweg 9, 2629 HZ Delft, The Netherlands

Supporting Information

ABSTRACT: Semiconductor films that allow facile ion transport can be electronically doped via electrochemistry, where the amount of injected charge can be controlled by the potential applied. To apply electrochemical doping to the design of semiconductor devices, the injected charge has to be stabilized to avoid unintentional relaxation back to the intrinsic state. Here, we investigate methods to increase the stability of electrochemically injected charges in thin films of a wide variety of semiconductor materials, namely inorganic semiconductors (ZnO NCs, CdSe NCs, and CdSe/CdS core/shell NCs) and organic semiconductors (P3DT, PCBM, and C_{60}). We show that by charging the semiconductors at elevated temperatures in solvents with melting points above room temperature, the charge stability at room temperature increases greatly, from seconds to days. At reduced temperature (−75 °C when using succinonitrile as electrolyte solvent) the injected charge becomes entirely stable on the time scale of our experiments (up to several days). Other high melting point solvents such as dimethyl sulfone, ethylene carbonate, and poly(ethylene glycol) (PEG) also offer increased charge stability at room temperature. Especially the use of PEG increases the room temperature charge stability by several orders of magnitude compared to using acetonitrile. We discuss how this improvement of the charge stability is related to the immobilization of electrolyte ions and impurities. While the electrolyte ions are immobilized, conductivity measurements show that electrons in the semiconductor films remain mobile. These results highlight the potential of using solidified electrolytes to stabilize injected charges, which is a promising step toward making semiconductor devices based on electrochemically doped semiconductor thin films.

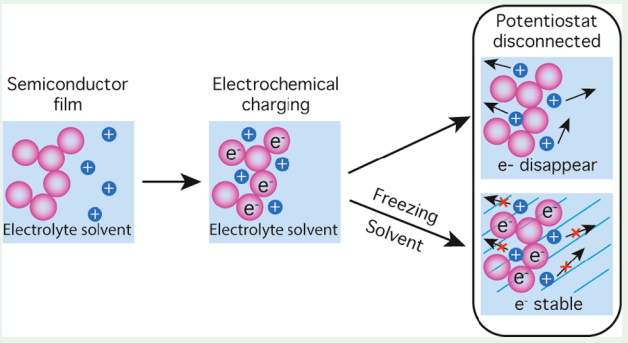

KEYWORDS: *electrochemistry, quantum dots, semiconductor films, room temperature freezing, doping stability, semiconductor devices*

INTRODUCTION

Over the past decades, several new promising semiconductor materials have emerged, including quantum dots (QDs), conductive polymers, fullerenes, and other small organic semiconductors. These materials are known for their cheap synthesis and tunable optical properties.[1−7] A general feature of the greatest importance for semiconductor devices is to control the charge carrier density. The above-mentioned materials have in common that the charge carrier density is not easily tuned via methods of impurity doping that have been developed for bulk inorganic semiconductors such as silicon.[8−10] However, as we show below, these semiconductor materials can all be doped efficiently using electrochemistry.

For electrochemical doping, a semiconductor film is deposited on a conductive electrode that forms the working electrode in an electrochemical cell, and charge is injected into the material from a counter electrode. To neutralize the injected charge, electrolyte cations of the opposite charge diffuse into the film and act as external dopants (Figure 1).[11] Because of the efficient nanoscale charge compensation, it is possible to reach extremely high doping densities of up to 10^{21} cm^{-3}.[12] In addition, since the electrolyte ions are external dopants that are typically not incorporated into the semiconductor materials itself, they do not lead to a disruption of the crystal lattice or molecular structure. Additionally, as the ions are stable in the ionized form (e.g., Li^+ would only reduce to Li at very negative electrochemical potentials), there is no problem with the activation of dopants, as is the case e.g. for common p-type impurity doping in II−VI semiconductors.[13] The same point implies that electrochemical doping does not

Received: May 8, 2019
Accepted: July 16, 2019
Published: July 16, 2019

DOI: 10.1021/acsanm.9b00863
ACS Appl. Nano Mater. 2019, 2, 4900−4909

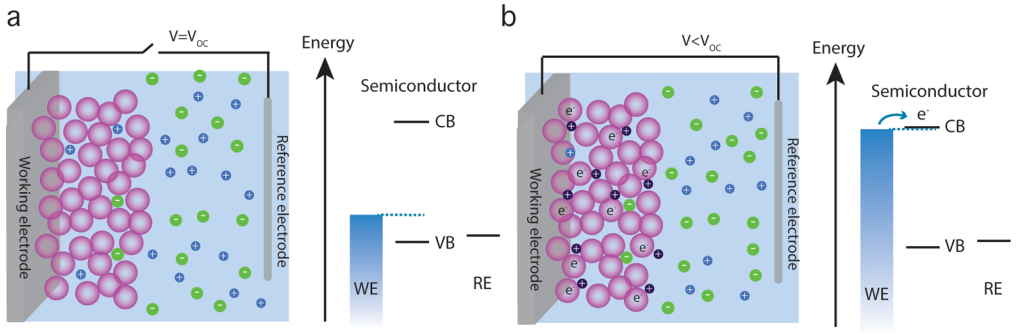

Figure 1. Schematic of electrochemical charge injection into a semiconductor film. (a) When no potential is applied to the WE, the Fermi level is inside the band gap of the semiconductor. (b) When a negative potential is applied to the WE compared to the RE, the Fermi level moves to the conduction band of the semiconductor which leads to electron injection. To neutralize the charge, electrolyte cations diffuse into the pores of the film.

introduce states in the bandgap that could act as recombination centers for electrons and holes, as is the case for substitutional impurity doping. Finally, the amount of the injected charge and thus the placement of the Fermi level are easily controlled with the touch of a button on the potentiostat.[12,14,15]

Electrochemical measurements have been used to investigate many different QDs and organic semiconductors.[12,16−20] Such electrochemically doped films could also be ideal for use in devices. A particularly interesting example of such a device that employs electrochemical doping is the light-emitting electrochemical cell (LEC). LECs are made by an electroluminescent semiconductor, most often a conjugated polymer, sandwiched between a cathode and an anode. The semiconductor layer also includes an ionic transport medium and electrolyte ions, and by applying voltages higher than the band gap energy of the semiconductor, one can create a p−n junction diode.[21−24] However, when the voltage source is disconnected, it is invariably observed that the injected charge disappears, both in the case of charged QD films[14] and in polymer LECs.[25] As will be discussed in detail below, the loss of charge density can be due to electrochemical reactions with impurities or intrinsic electrochemical reactions with the material itself. Moreover, when used in junctions, potential differences can lead to diffusion of the dopant ions, resulting in a change of the charge density.

Several approaches have been used to increase the room temperature doping stability in LECs. One way is to reduce ion transport in the electrolyte solvent. Tang et al. polymerized the electrolyte with the counterions,[26] and Wantz et al. used polymer electrolytes with high glass transition temperatures.[27] Another way is to chemically fix the electrolyte counterions. To do so, Hoven et al. used a cationic conjugated polyelectrolyte containing fluoride counteranions, with an underlayer of a neutral conjugated polymer that had anion trapping functional groups.[28]

Despite intense studies, complete doping stability has not been achieved at room temperature. Gao et al. made a stable LEC at 100 K, which freezes the electrolyte solvent.[22] At this temperature, the electrolyte solvent is frozen, and both external dopants and impurities are immobilized. In addition, electrochemical side reactions of the semiconductor material itself are slowed down. Similarly, Guyot-Sionnest et al. and Houtepen et al. showed that the charge density in different quantum dots (CdSe, PbSe, and ZnO nanocrystals) and organic polymers (poly(*p*-phenylenevinylene, PPV) is stable for days at cryogenic temperatures in various electrolyte solvents.[29−32]

Here we investigate the possibility of stabilizing electrochemically doped semiconductor films at room temperature using a large variety of electrolyte solvents with melting points above room temperature (RT). The charge is injected into the system when the solvent is liquid. The system is then cooled to room temperature, causing the solvent to freeze. This could enable the use of electrochemically doped semiconductor devices at room temperature.

In this work we show electrochemical doping for three different QD materials (ZnO, CdSe, and CdSe/CdS QDs), two fullerenes (C_{60} and PCBM), and two conductive polymers (P3DT and P3HT). We investigate how stable the doping is by measuring the electrochemical potential over time for different electrolyte solvents at different temperatures. When using acetonitrile as the electrolyte solvent, for CdSe, CdSe/CdS QDs, and PCBM it takes <30 s for the electrochemically injected electrons to spontaneously leave the conduction band, even under stringent anaerobic conditions. By use of a ZnO QD film in a succinonitrile supporting electrolyte, which has a melting point of 57 °C, charge stability at RT is improved by 2 orders of magnitude. When the temperature is decreased to −75 °C, the injected electrons become entirely stable on the time scale of our experiments (hours to days) and cannot be removed even by applying positive potentials, showing that the cations that compensate for the electrons have become immobilized.

In a search for a similar improved charge stability at RT, we have investigated a range of different electrolyte solvents with melting points above room temperature. All solvents showed improved RT charge stability compared to acetonitrile; the best results were obtained for poly(ethylene glycol) (PEG) with molecular weight ≥4000. In that electrolyte solvent injected charges remained in the conduction or valence band for over an hour at RT for all materials. Optimized measurements on ZnO NCs show that even after several days the Fermi level remained in the conduction band.

EXPERIMENTAL METHODS

Materials. Zinc acetate dihydrate ($Zn(CH_3COO)_2{\cdot}2H_2O$ reagent grade), potassium hydroxide (KOH pellets), cadmium acetate ($CdAc_2$, 99.999%, ChemPur), oleic acid (OA, 90%), 1-octadecene (ODE, 90%), selenium powder (Se, ChemPur), trioctylphosphine (TOP, 90%), trioctylphosphine oxide (TOPO, 99%), octadecylamine (ODA, 90%), oleylamine (OLAM, 70%), 1-octanethiol (≥98.5%), 1,4-butanedithiol (BDT, 97%), poly(3-decylthiophene-2,5-diyl)

DOI: 10.1021/acsanm.9b00863
ACS Appl. Nano Mater. 2019, 2, 4900−4909

(P3DT, regioregular), poly(3-hexylthiophene-2,5-diyl) (P3HT, regiorandom), phenyl-C_{61}-butyric acid methyl ester (PCBM, 99%), fullerene (C_{60}, 99.9%), 1,2-dichlorobenzene (99%), chlorobenzene (99.8%), indium-doped tin oxide substrates (ITO, PGO Germany), lithium perchlorate ($LiClO_4$, 99.99%), ferrocene (Fc, 98%), decamethylferrocene (97%), anhydrous ethylene carbonate ($(CH_2O)_2CO$, 99.8%), succinonitrile (99%), dimethyl sulfone (98%), poly(ethylene glycol) (PEG M_n of 600, 4000, 6000, 8000, 20000, and 35000), and anhydrous solvents (acetonitrile, 99.99%, methanol, 99.8%, ethanol (maximum 0.01% H_2O), toluene, 99.8%, hexane, 95%, and butanol, 99.8%) were all purchased from Sigma-Aldrich unless stated otherwise. Acetonitrile was dried before use in an Innovative Technology PureSolv Micro column. All other chemicals were used as received.

ZnO QD Synthesis. The ZnO QDs were synthesized as previously described.[17] 3.425 mmol of zinc acetate dihydrate and 50 mL of ethanol were combined at 60 °C in an Erlenmeyer flask. A potassium hydroxide mixture (6.25 mmol of KOH in 5 mL of methanol) was added dropwise to the stirred zinc acetate−dihydrate mixture. After an additional 1 min in reaction time, the heat source was removed. The QDs were purified by the addition of hexane, and the flocculates were isolated by centrifugation at 2000 rpm for 1 min. The QDs were redissolved in ethanol, and the dispersion was stored at −20 °C to avoid further growth by Ostwald ripening.

CdSe QD Synthesis. The CdSe QD cores were synthesized according to the procedure of Qu et al.[33] The Cd precursor containing 0.66 g of $CdAc_2$, 3.68 g of OA, and 25.9 g of ODE was degassed for 3 h. For the Se precursor, 1.42 g of Se powder was dissolved at 200 °C in 7.5 g of TOP and 11.9 g of ODE. 1.11 g of TOPO, 3.2 g of ODA 90%, and 5.2 g of the Se precursor were added to a three-neck round-bottom flask and heated to 300 °C. At 300 °C, 4.9 g of the Cd precursor was injected into the bottle. The reaction was kept at around 280 °C for 9 min and cooled by an air gun. When the solution reached 100 °C, it was quenched with 5 mL of anhydrous toluene. The CdSe particles were precipitated by addition of methanol and butanol in a 1:1:1 crude solution:anhydrous methanol:anhydrous butanol ratio. The flocculates were isolated by centrifugation at 2800 rpm for 8 min and redissolved in toluene.

CdSe/CdS Shell Growth. The CdS shell growth was synthesized by a known procedure.[34] 400 nmol of CdSe QDs in toluene was combined with 3 mL of OLAM and 4 mL of ODE and degassed for 1 h at room temperature and for 20 min at 120 °C under vacuum. The reaction solution was heated to 310 °C under N_2, and when the temperature reached 240 °C, the Cd precursor (as in the core synthesis, desired amount diluted in 1 mL of ODE) and 1-octanethiol (1.2 equiv amounts to Cd oleate diluted in 3.4 mL of ODE) are injected dropwise into the reaction solution at the rate of 1 monolayer per hour by syringe pumps. When the injection is finished, 1 mL of oleic acid was injected, and the NCs were annealed at 310 °C for an hour. Afterward, the solution was cooled to 50 °C. The CdSe/CdS QDs were precipitated by the addition of butanol and methanol and centrifuged at 3800 rpm for 5 min. The QDs were redissolved in hexane.

Film Preparation. All films were prepared on two different working electrodes (WE), on indium-doped tin oxide (ITO) substrates, or on home-built interdigitated gold electrodes (IDEs). The IDE is a glass substrate containing four different gold working electrodes prepared by optical lithography. The four working electrodes provide four different sensitivities in the measurements. See Figure S1 in the Supporting Information for more details.

ZnO QD films were drop-casted in air and annealed for 1 h at 60 °C.

CdSe and CdSe/CdS films were made by the layer-by-layer dip-coating procedure in a nitrogen-filled glovebox. The substrate was immersed in a QD dispersion for 30 s and thereafter in a solution containing 0.2 M 1,4-butanedithiol cross-linking ligands in methanol for 30 s; ultimately, it was dipped in methanol to rinse excess ligands.

For P3DT film preparation, 10 mg of P3DT was dissolved in 1 mL of 1,2-dichlorobenzene. The substrate was coated by spin-coating for 60 s at 3000 rpm with a ramp of 1000 rpm/s.

For PCBM films, 50 μL of 3 wt % PCBM chlorobenzene solution was spin-coated for 45 s at 3000 rpm with a ramp of 1000 rpm/s. The substrate was placed on a hot plate at 100 °C for 10 min to ensure the evaporation of chlorobenzene.[35]

C_{60} films were prepared by a physical vapor deposition technique using an AJA ATC Orion evaporator at high vacuum ($\leq 1 \times 10^{-6}$ mbar). The C_{60} powder was placed in a crucible and heated to sublimation temperature. The temperature was kept fixed during the evaporation.[36]

Electrochemical Measurements. All electrochemical measurements were performed in a nitrogen-filled glovebox with moisture ≤0.5 ppm and O_2 levels ≤0.1 ppm. The measurements were performed with an Autolab PGSTAT128N potentiostat with a bipotentiostat BA module. Two different three-electrode electrochemical cells were used (Figure S2). The former one was a cuvette cell where the sample was deposited on a WE and immersed in a $LiClO_4$ electrolyte solution. The solution further contained a Ag pseudo-reference electrode (RE) and a Pt sheet as a counter electrode (CE). The latter electrochemical cell was a flat cell containing a well where the sample on the WE was placed inside the well and the solvent was placed on top of the sample. On top of the solvent a glass substrate was placed containing a Ag pseudo-RE and a Pt mesh CE (see Figure S3). It was made sure both the RE and the CE touched the solvent but not the WE to avoid short-circuiting. The flat cell is used when smaller volumes of solvents are needed or when the solvents are very viscous.

Both cell designs were used for cyclic voltammetry measurements (CVs) for different semiconductor materials. The CVs were performed in a $LiClO_4$ electrolyte solution starting from the open circuit potential (V_{oc}) of the material. The potential was scanned at 50 mV/s in the positive/negative direction until charge was injected into the valence/conduction band of the material. The CVs were repeated three times.

Before the measurements, the Ag pseudo-reference electrode was calibrated with a ferrocene/ferrocenium couple[37] (cuvette cell) or a decamethylferrocene/decamethylferrocenium couple (flat cell).[38] The difference between the decamethylferrocene/decamethylferrocenium and the ferrocene/ferrocenium couple was measured as 0.57 V. All potentials are given versus the ferrocene/ferrocenium couple.

Spectroelectrochemical Measurements. The absorbance changes in the spectroelectrochemical measurements were measured as a function of the applied electrochemical potential with a fiber-based UV−vis spectrometer (Ocean Optics USB2000) using an Ocean Optics DH 2000 lamp as a light source.

Source-Drain Electronic Conductance Measurements. Source-drain electronic conductance measurements were performed as previously described by the use of the home-built IDE.[17] During the measurements, two WEs were used in a source-drain configuration; the source-drain gap width was 25 μm while the gap length was 6.8 cm. The potential is stepped, and after the system reached equilibrium, the potential of WE1 was scanned in a CV manner around the fixed potential of WE2 with a difference of ±10 mV. The slope of the current versus the potential gives the conductance, G. From the conductance, the conductivity, σ, can be calculated via eq 1.

$$\sigma = \frac{G \times w}{l \times h} \tag{1}$$

where w is the source-drain width, l is the gap length, and h is the height of the sample.

Fermi-Level Stability Measurements. Fermi-level stability measurements were performed by following a procedure similar to Pei et al.[25] The measurements were performed after charge injection into the conduction band or the valence band of the different semiconductors. When equilibrium was reached, the CE was disconnected from the WE and the RE electrode. By doing so, no additional charge can be injected into the film while the potential between the WE and the RE is measured. This potential is equal to the Fermi level of the working electrode vs the Fermi level of the reference electrode. If injected charges leave the semiconductor, this

DOI: 10.1021/acsanm.9b00863
ACS Appl. Nano Mater. 2019, 2, 4900−4909

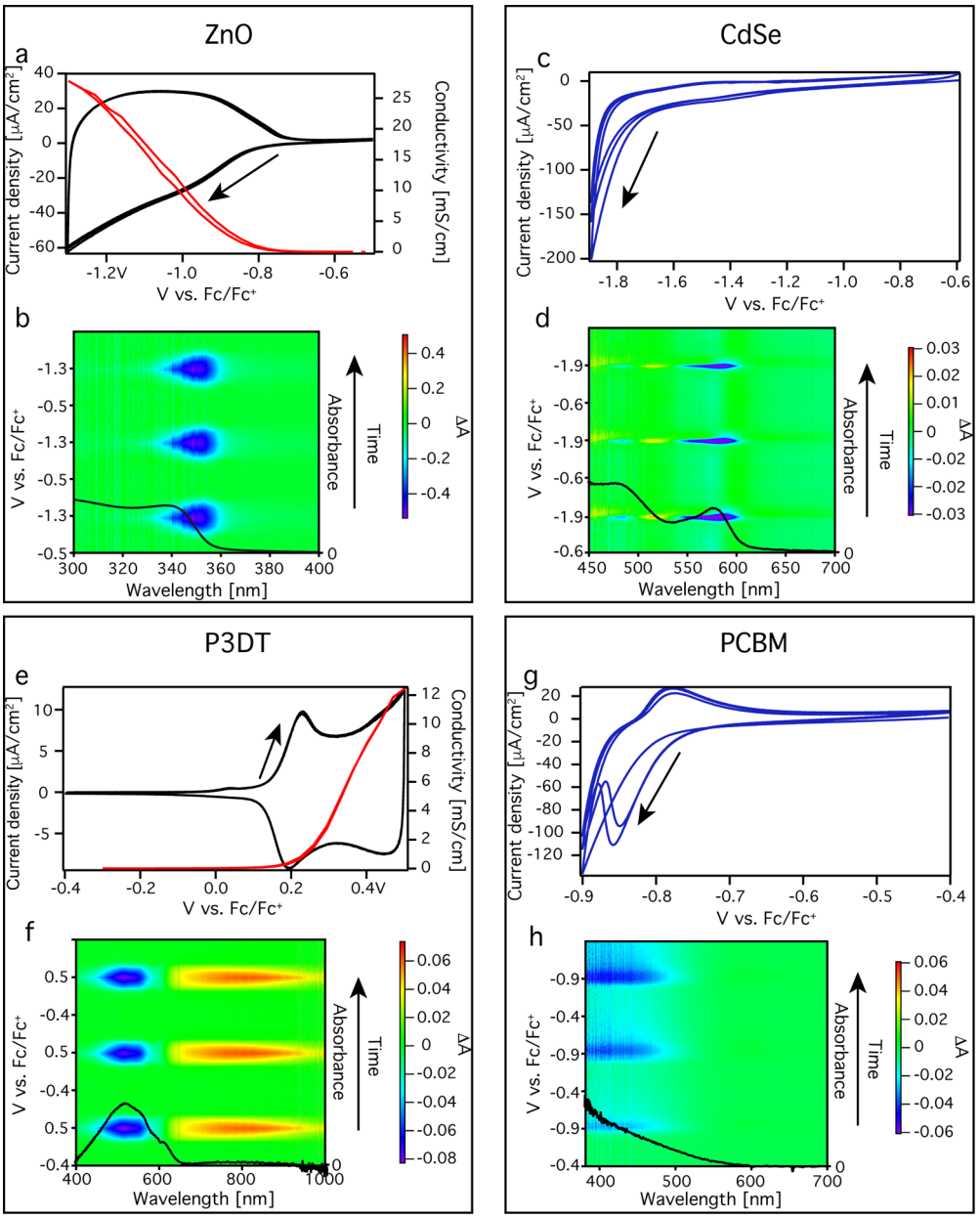

Figure 2. Spectroelectrochemical measurements for different semiconductor films. (a), (c), (e), and (g) show the CVs (black or blue trace) for a (a) ZnO QD film, (c) CdSe QD film, (e) P3DT film, and (g) PCBM film. The measurements are performed on an ITO substrate in 0.1 M $LiClO_4$–acetonitrile solution with a scan speed of 50 mV/s. The scans start at the V_{oc} of the system and are repeated three times; the arrows indicate the scan directions. (a) and (e) furthermore show the source-drain electronic conductivity in red. (b), (d), (f), and (h) show the change in absorbance during the three scans. The color plot includes the absorbance of the film. A negative change in absorbance is shown in blue, and a positive change is shown in red.

will result in a drop of the Fermi level and a change in potential. When solvents that are solid at room temperature are used, the sample is charged at elevated temperature when the solution is liquid, after which the temperature is decreased while the same potential is applied. When the desired temperature is reached, the CE is disconnected from the WE and the RE.

RESULTS AND DISCUSSION

Figure 2 shows spectroelectrochemical measurements on ZnO QDs, CdSe QDs, P3DT, and PCBM performed inside a glovebox, where electrochemical charge injection takes place. Spectroelectrochemical measurements for CdSe/CdS core/shell QDs, P3HT, and C_{60} are shown in Figures S4 and S5. For comparison, a CV of a blank ITO is shown in Figure S6. For all films it is observed that as the potential is changed into the conduction band (QDs and fullerenes) or valence band (conducting polymers), the current increases, the band edge absorbance decreases, and the conductivity increases drastically (measured in the case of ZnO and P3DT).[29,39] We also show for ZnO QD films that this is accompanied by an increase of absorption in the IR due to intraband absorption of the injected charges (Figure S7). All these effects are a clear demonstration of charge injection into the conduction or valence band of the semiconductors.

From Figure 2 it is clear that the CVs of P3DT and ZnO are almost symmetric.[40] Charge injection for CdSe and PCBM is not as reversible; when the scan is reversed, only a small

DOI: 10.1021/acsanm.9b00863
ACS Appl. Nano Mater. 2019, 2, 4900−4909

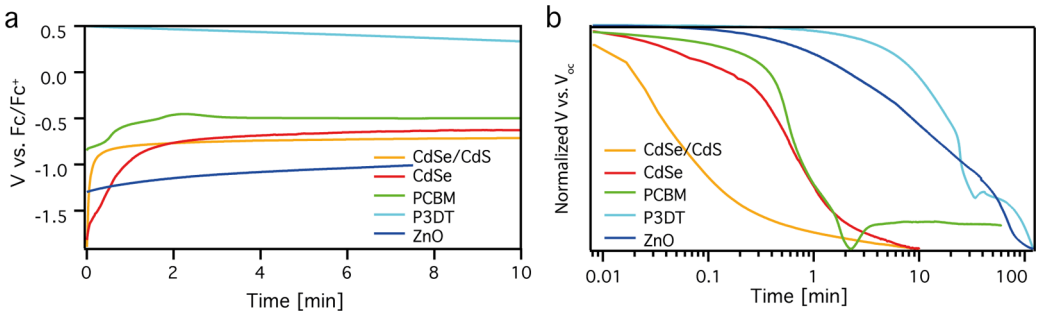

Figure 3. Fermi-level stability measurements for different semiconductor films. (a) Fermi-level stability measurements for the semiconductors in 0.1 M $LiClO_4$–acetonitrile electrolyte solution for the duration of 10 min. The injected charge gradually leaves all semiconductor films. (b) The same measurements as in (a) with the normalized initial potential after the V_{oc} is set as 0.

Table 1. Melting Points of Electrolyte Solvents

solvent	acetonitrile	ethylene carbonate	succinonitrile	PEG 6000	dimethyl sulfone
melting point (°C)	−45	37	57	56–63	109

positive current can be seen in the CVs. This means that the injected electrons are not extracted.[14] This is a first sign of the instability of injected charges.

Similar electrochemical measurements have been used in the literature as a means to study the optical and electrical properties of semiconductor thin films.[14,41−45] However, here we want to investigate whether electrochemical doping can also be used to prepare doped films that can be used in semiconductor devices. Hence, we investigate next how long the injected charge remains if the potentiostat is disconnected.

To determine the stability of electrochemically injected charge the counter electrode is disconnected and the potential of the working electrode (with respect to the reference electrode) is recorded over time (see the Experimental Methods section). Similar measurements have been performed before by Pei et al. for LECs.[25] We call this experiment a Fermi-level stability measurement. If the injected electrons or holes leave the system, the potential will change from the initially applied potential value (just before disconnecting the CE) back to the original V_{oc}. By simultaneously recording the absorption bleach, we verified that we are indeed measuring the potential of the working electrode correctly with such a Fermi-level stability measurements (Figure S8)

Figure 3a shows Fermi-level stability measurements for all investigated semiconductor films in 0.1 M $LiClO_4$–acetonitrile solutions. For comparison, Fermi-level stability measurements normalized to 1 at the potential set before disconnecting the counter electrode and to 0 at the initial V_{oc} are shown in Figure 3b. For CdSe, CdSe/CdS QDs, and PCBM it takes <35 s for the potential to be half of the maximum. In contrast, for ZnO QDs and P3DT it takes ∼14 and ∼23 min, respectively. Both ZnO and P3DT are clearly much more stable than the other systems, in line with the more symmetric CVs for these materials in Figure 2.

The loss of charge density and potential shown in Figure 3 is similar to self-discharge in batteries.[46] We consider three possible causes for the observed loss. First of all, impurities can extract the charges from the conduction/valence band of the material. The most common impurity is molecular oxygen, which can be reduced to its radical anion superoxide by electrons in the conduction band of the semiconductor materials. Indeed, performing the same experiments for ZnO QDs outside the glovebox results in much less symmetric CVs and a rapid loss of electrons (Figure S9). While the glovebox atmosphere contains ≲0.1 ppm oxygen, on time scales of minutes to hours this may still lead to significant reactions with electrons.

Second, intrinsic electrochemical reactions can occur with the material itself.[14] The strong differences between e.g., ZnO QDs and CdSe QDs in Figures 2 and 3 hint toward a strong contribution of intrinsic reduction reactions in the latter material. Such reactions have been observed and discussed before and have sometimes been assigned to the reduction of surface Cd^{2+} to Cd^0.[47−50] However, the occurrence and nature of such surface electrochemical reactions, and their potential reversibility, are largely unknown.

Finally, movement of counterions can lead to the loss of injected charges. This process should not occur spontaneously as the counterions are Coulombically bound to the injected charge carriers and should not diffuse out of the film unless there is another mechanism (i.e., the first two mechanisms above) that removes the injected charge carriers. However, if electric fields are present, as is the case in any semiconductor junction or any device under operation, they will cause counterions to migrate with an associated loss of injected charge carrier density.

To make a permanently doped semiconductor system by means of electrochemistry, which can also be used in a device, these processes need to be controlled. As was discussed above, several methods have been explored to make stable LECs at room temperature.[26−28] While an increase in doping stability was achieved, none of these methods proved successful in fully stabilizing the charge density at room temperature. Until now, the only successful way of obtaining truly stable electrochemical charge injection has been at cryogenic temperatures.[22,29−31,51] This is clearly not suitable for real-world applications. However, freezing does not necessarily require low temperatures.

Want et al. used polymer electrolyte solvents with higher glass transition temperatures and gained a higher stability at room temperature for conductive polymer LECs; however, the devices decayed and were undoped after 100 h.[27] However, many other types of solvents have proven to be good electrolyte solvents for either fuel cells or batteries.[52−55] We sought solvents that are chemically similar to common

DOI: 10.1021/acsanm.9b00863
ACS Appl. Nano Mater. 2019, 2, 4900−4909

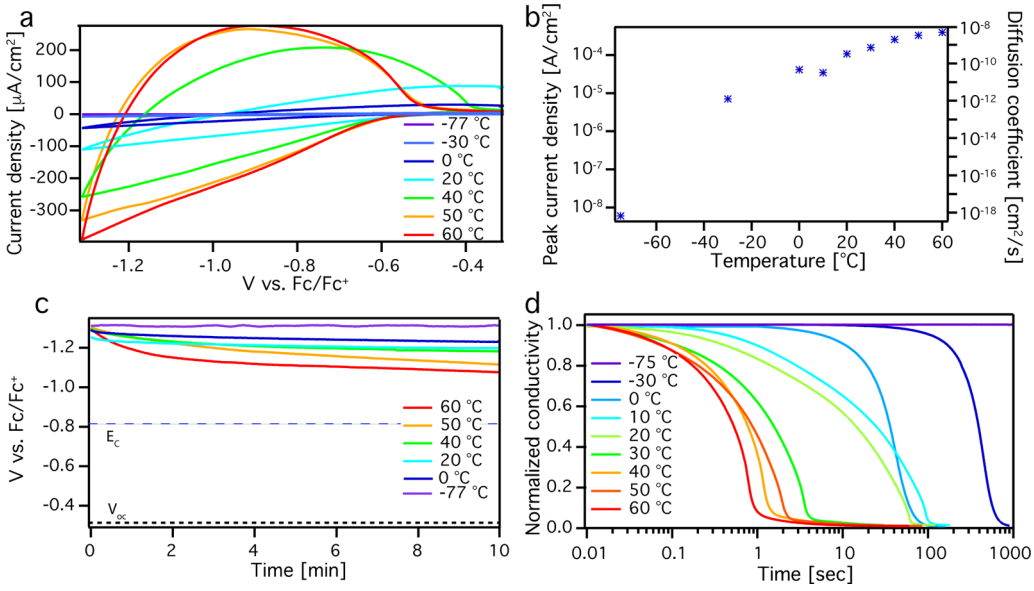

Figure 4. Electrochemical measurements for a ZnO QD film in succinonitrile performed at temperatures between −77 and 60 °C. (a) CVs at different temperatures. The potential is scanned between −0.36 and −1.36 V at 50 mV/s scan rate. (b) The peak current obtained from the CVs for different temperatures (left axis) and the corresponding diffusion coefficient (right axis). Both of them are plotted with the same symbol (blue stars). By lowering the temperature, the Li^+ diffusion coefficient decreases due to the solidifying of the solvent. (c) Fermi-level stability measurements performed at different temperatures. The graph includes the conduction band edge (E_C, blue dashed line) and the open circuit potential of the ZnO QD film (V_{OC}, black dashed line) When the temperature is decreased, the potential becomes much more stable. (d) Conductivity measurements after a potential step from −1.36 to −0.36 V. The initial conductivity at each temperature is normalized. The conductivity drops as a result of electrons that leave the ZnO QDs film upon discharging. At lower temperatures discharging becomes much slower and stops altogether at −75 °C.

electrolyte solvents but with higher melting points (see Table 1).

We use ZnO as a model system due to its stable and reversible electrochemistry, as highlighted in Figures 2 and 3, but the results are general and many of the measurements are shown for the other semiconductor materials either in the text or in the Supporting Information. Figure 4a shows CVs for a ZnO QD film on an ITO electrode in 0.1 M $LiClO_4$ in succinonitrile electrolyte solution at temperatures between −77 and 60 °C. It is clear that by lowering the temperature, the current density decreases, and the positive peak current density occurs at more positive potentials. Both of these observations can be explained by the reduced diffusion of the electrolyte ions as the temperature decreases. At −77 °C, no features are seen in the CV and no charging occurs (see Figure S10).

Figure 4b shows the peak current density obtained from the CVs at −1.36 V at different temperatures (left axis). As we showed in detail recently,[17] charge injection is limited by counterion diffusion. Under these conditions it is possible to estimate the diffusion coefficient of the Li^+ cation at each temperature with the Randles−Sevcik equation:

$$j_p = 0.4463nFC^*\left(\frac{nFvD}{RT}\right)^{1/2} \quad (2)$$

where j_p is the peak current density, n is the number of electrons, F is the Faradaic constant, C^* is the concentration of the electrolyte, v is the scan rate, D is the diffusion coefficient, R is the gas constant, and T is the temperature. The resulting estimated diffusion coefficient values are plotted versus the right axis in Figure 4b. By cooling from 60 to 20 °C, the cation diffusion coefficient reduces by an order of magnitude. At −77 °C, the cation diffusion coefficient is estimated to be 10^{-18} cm^2/s, 10 orders of magnitude lower than at 60 °C. With such a diffusion coefficient it would take a Li^+ ion ∼10^{10} s (= 450 years) to diffuse out of a 1 μm thick ZnO NC film. This shows that by freezing the electrolyte solvent, the diffusion coefficient of the Li^+ cation decreases greatly, which should lead to increased electron stability after charge injection. At the same time, freezing the electrolyte should also prevent impurity diffusion, which will also increase the stability of doped semiconductor films.

For the same sample, Fermi-level stability measurements were performed for the duration of 10 min. The results are shown in Figure 4c. Measurements on a longer time scales are shown in Figure S11. A potential of −1.36 V vs ferrocene is applied to the sample at temperatures where charge injection can occur (around 60 °C). While continuously applying this potential, the temperature is lowered to the desired temperature, where the Fermi-level stability measurements are initiated. For measurements performed at temperatures above the melting point of succinonitrile, a significant increase in potential is observed on the time scale of minutes. By lowering the temperature, the potential increases more gradually. At RT it takes around 145 min for the potential to reach the value of −1.17 V vs ferrocene (the whole measurement is shown in Figure 5a), while in acetonitrile the same potential is reached after only 92 s. However, while the RT charge stability is much higher when using succinonitrile as a solvent, it is not until −77 °C that the injected electrons are entirely stable for at least 10 min. This indicates that complete crystallization of the solvent in the crowded pores between the QDs where the cation concentration is high is much more difficult, resulting in a very strong melting point depression.

In the Fermi-level stability measurements no electric field is applied, and the electrons leave the semiconductor sponta-

DOI: 10.1021/acsanm.9b00863
ACS Appl. Nano Mater. 2019, 2, 4900−4909

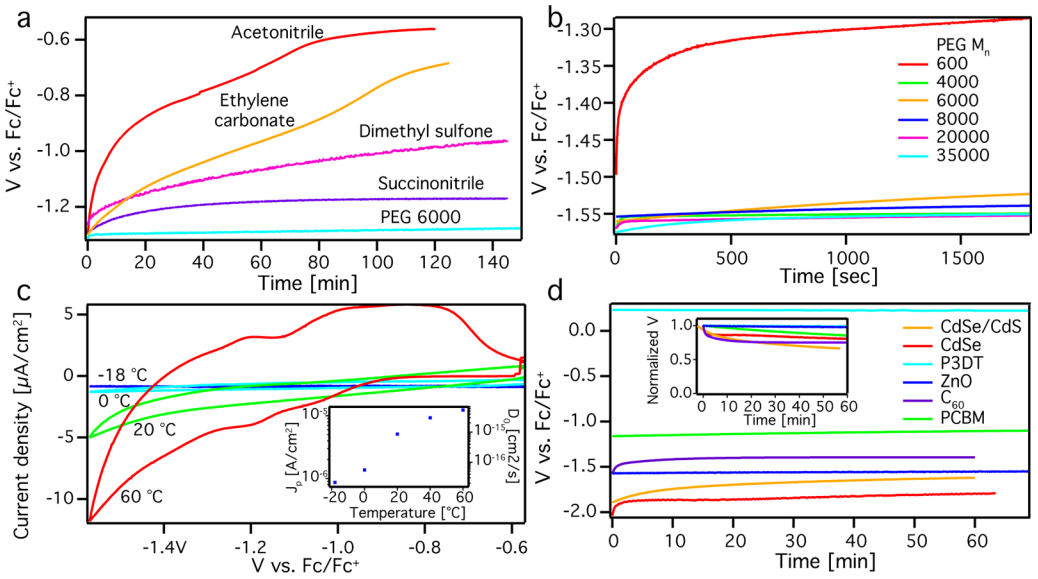

Figure 5. Electrochemical measurements performed with different electrolyte solvents. (a) Fermi-level stability measurements for a ZnO QD film in different electrolyte solvents with different melting points measured at room temperature. (b) Fermi-level stability measurements for a ZnO QD film measured in PEG with different number-average molecular weights, M_n (from 600 to 35000) at room temperature. (c) CVs for a ZnO QD film in 11 wt % $LiClO_4$ PEG 6000 performed at temperatures between −18 and 60 °C. The figure includes an inset containing the peak current density, J_p (left axis), and the calculated Li^+ diffusion coefficient, D_0 (right axis), versus the temperature. (d) Fermi-level stability measurements for different semiconductor systems in an 11 wt % $LiClO_4$ in either PEG 4000 or PEG 6000 electrolyte solvent. The panel includes an inset where the initial V_{oc} is set as a 0 and the measured potential has been normalized. It takes longer than an hour for the injected charge to leave the conduction/valence band of the materials.

neously, through reacting either with impurities or via intrinsic surface electrochemical reactions. However, in devices electric fields are present which could cause ions to migrate and the doping density to change. To investigate this, we actively apply a potential close to the original V_{oc} after charging the sample. This change in potential will force ions out of the film via migration, if they are mobile, and will cause discharging of the film. However, if ions are immobile, such discharge should be prevented. This process hence depends on ion mobility and not on reactions with impurities or intrinsic surface electrochemical reactions.

Figure 4d shows normalized source-drain conductivity measurements of a ZnO QD sample on an IDE. In the measurement, a potential of −1.36 V is applied to the ZnO QDs when the solvent is liquid (around 60 °C) and then the temperature is lowered, and at the desired temperature the potential is changed to the original V_{oc} (−0.36 V) while the source-drain current is recorded. Because the conductance depends linearly on the electron concentration, this measurement detects the drop in charge density in a sensitive way. At 60 °C, when succinonitrile is liquid, it takes <1 s to discharge the film, while at −30 °C it takes ∼1000 s. At −75 °C the conductivity does not drop at all, showing that at this temperature the electrolyte cations are immobilized in the frozen solvent.

The temperature-dependent source-drain conductance is shown in Figures S12 and S13. From those figures and from Figure 4d it is clear that even at −75 °C, when the ions are immobilized and the film cannot be discharged, electrons can still move between the ZnO QDs. This is a crucial requirement for using such electrochemically doped films in devices.

By looking at the temperature-dependent potential and discharging results (Figures 4c and 4d), it is clear that even when succinonitrile is well below its reported melting temperature (57 °C), diffusion of ions and impurities is still possible. Apparently, the solvent does not properly freeze until at −75 °C, a surprising 132 °C lower than the reported melting point of succinonitrile. Differential scanning calorimetry shows only around 30 °C melting point depression for 0.1 M $LiClO_4$−succinonitrile (Figure S14), and furthermore both solvents are solid at room temperature. Further melting point depression is most likely caused by the inability of the solvent to crystallize in a crowded environment of the nanopores in the QD film. Because of these factors, electrolyte solvents with higher melting points than succinonitrile are most likely better suited.

To investigate whether an even larger improvement of the RT charge stability is possible, measurements with other electrolyte solvents were performed. Figure 5a shows Fermi-level stability measurement for ZnO QD films with $LiClO_4$ in acetonitrile, ethylene carbonate, dimethyl sulfone, succinonitrile, and PEG 6000 at room temperature. It is clear that poly(ethylene glycol) (PEG) offers the greatest RT charge stability. After 170 min, the potential of the ZnO QD film in PEG has increased from −1.30 to −1.273 V while it only takes 11 s for a ZnO QD film to reach this potential in acetonitrile. We observe that PEG has a lower melting point than dimethyl sulfone (56−63 °C vs 109 °C) but shows a much better charge stability. We hypothesize that the better stability in PEG can be caused by the combination of high viscosity, resulting in slower diffusion of impurities, and by a lower impurity solubility.

As both the viscosity and the melting point increase with increasing PEG chain length, Fermi-level stability measurements were performed with PEG with number-average molecular weights, M_n, between 600 and 35000 (Figure 5b). Of these only PEG 600 is liquid at room temperature, and it shows the most rapid change in the measured potential. This confirms our conclusion above that solidifying the electrolyte is

DOI: 10.1021/acsanm.9b00863
ACS Appl. Nano Mater. 2019, 2, 4900−4909

a promising strategy to create permanently doped nanocrystal films with electrochemical doping. PEG 4000 was chosen for Fermi-level stability measurements with a ZnO QD sample over a weekend (Figure S15). After 65 h, the potential had only increased by 0.2 V (to −1.35 V), which is still 0.55 V more negative than the conduction band edge of the ZnO QDs. The sample thus remained degenerately doped after several days. Wantz et al. used polymer electrolytes with different glass transition temperatures for conductive polymer LECs and tested their stability at room temperature. Their best operation half-lifetime at room temperature was between 10 and 20 h.[27] A direct comparison to this half-lifetime of LEC operation is difficult, but it appears the doping stability with the present approach is better.

To investigate the diffusion of counterions in PEG in more detail, CVs were performed on a ZnO QD film in 11 wt % $LiClO_4$ PEG 6000 solution at temperatures between −18 and 60 °C (Figure 5c). These CVs show a much larger separation between forward and backward peaks than for succinonitrile (Figure 4a), in line with the higher viscosity of PEG and the associated smaller diffusion coefficient of Li^+ in that solvent. By lowering the temperature, the peak current density decreases and the peak separation increases further. Using eq 2, we find that the diffusion coefficient of Li^+ in PEG 6000 (inset of Figure 5c) is a few orders of magnitude lower than in succinonitrile (10^{-14} cm^2/s vs 10^{-8} cm^2/s, both at 60 °C). Similar measurements were performed for a P3DT film in 11 wt % PEG 6000 and show the same trend (Figure S16).

Fermi-level stability measurements with solvents from Table 1 were also performed for CdSe QDs, CdSe/CdS QDs, P3DT, PCBM, and C_{60} (Figure S17). In all cases, the stability of injected charges is better when solvents with melting points above room temperature are used and is best when using PEG with $M_n \geq 4000$. An overview of the charge stability for all systems in PEG is shown in Figure 5d. The figure includes an inset where the potential is normalized (the V_{oc} before charging is set to 0, and the initial applied potential is normalized to 1). When the results are compared to the measurements performed with acetonitrile (Figure 3), it is clear that for all materials the electrochemically injected charge is much more stable in PEG. As before, the potential is not completely stable as it gradually relaxes to the original V_{oc}, but a great enhancement is achieved. For all materials, charge is still present in the conduction/valence band after at least an hour.

While PEG proved to give the best charge stability at room temperature, likely due to a combination of the lowest impurity concentration and impurity diffusion coefficient, the overall best result was obtained for succinonitrile at −75 °C. We were not able to measure the charge stability in PEG at such low temperatures as going through the glass transition of PEG[56] resulted in a loss of contact to the electrodes. However, even if we could solve these experimental problems, we consider it is unlikely that PEG can crystallize into a very dense crystal structure required for the immobilization of counterions and impurities. This is evidenced by the fact that upon solidification the diffusion coefficient of Li^+ in PEG 6000 is reduced by about 2 orders of magnitude (Figure 5c), while for succinonitrile a reduction of 10 orders of magnitude is observed (Figure 4b). The diffusion coefficient of Li^+ in succinonitrile at −70 °C is $\sim 10^{-18}$ cm^2/s, which is 2 orders of magnitude below the lowest diffusion coefficient found for PEG6000 ($\sim 10^{-16}$ cm^2/s at −10 °C).

We are currently looking for other solvents, such as nitriles with even higher melting points than succinonitrile, to see whether we can extend the full stability of injected charges to room temperature. Additionally, the use of different ions than Li^+ might show a further reduction of the diffusion coefficient and a gain in stability.

CONCLUSIONS

In summary, we have shown electrochemical doping for a broad range of semiconductor films. In all cases, the injected charge disappears quickly when the films are disconnected from the external applied potential due to reactions with impurities and intrinsic electrochemical reactions at the surface of the semiconductors. For acetonitrile, the injected charge is stable for 37 min or less under stringent air-free conditions, and for some materials the stability lasts only a few seconds (CdSe and CdSe/CdS QDs). We have shown that this charge stability at room temperature is greatly improved for all investigated semiconductor films by charging the films at elevated temperature in different solvents with melting points above room temperature. In terms of room temperature charge stability, the best solvent was PEG with molecular weight of ≥4000, which increases the lifetime of injected charges to several days. Further improvements in charge stability should be possible as experiments at −75 °C in succinonitrile showed that the electrochemically injected charge becomes entirely stable on experimental time scales. In addition, we showed that the charge density is even stable under applied electric fields, as the electrolyte ions are not mobile in the frozen electrolyte. This shows that such films can be used in a range of different semiconductor devices, where internal electric fields are present.

ASSOCIATED CONTENT

Supporting Information

The Supporting Information is available free of charge on the ACS Publications website at DOI: 10.1021/acsanm.9b00863.

Home-built IDE, electrochemical cells, CE and RE electrode in flat cell, spectroelectrochemical measurements for CdSe/CdS, C60, and P3HT films, spectroelectrochemical measurements for C60 film with $TBAClO_4$, CV of a blank ITO, intraband absorbance in a ZnO QD film, differential absorbance during Fermi-level stability measurements, CVs for ZnO measured in air, CV for ZnO measured at −77 °C in succinonitrile, Fermi-level stability measurements at longer time scales, source-drain electronic conductance measurements, DSC measurements, Fermi-level stability measurements for ZnO QD film in PEG over a weekend, temperature-dependent CVs for P3DT, Fermi-level stability measurements in different solvents (PDF)

AUTHOR INFORMATION

Corresponding Author

*E-mail A.J.Houtepen@tudelft.nl.

ORCID

Solrun Gudjonsdottir: 0000-0002-4793-8747

Arjan J. Houtepen: 0000-0001-8328-443X

Present Address

§Utrecht University, Inorgani Chemistry and Catalysis, Universiteitsweg 99, 3584 CG Utrecht, The Netherlands.

DOI: 10.1021/acsanm.9b00863
ACS Appl. Nano Mater. 2019, 2, 4900−4909

Notes

The authors declare no competing financial interest.

■ ACKNOWLEDGMENTS

We acknowledge Kevin Felter for his help in making the C_{60} films, Jaco Geuchies for his help in the CdSe/CdS synthesis, and Youp van Goozen for his help in making both the cuvette and the flat cell setup. A.J.H. acknowledges support from the European Research Council Horizon 2020 ERC Grant Agreement No. 678004 (Doping on Demand).

■ REFERENCES

(1) Bailey, R. E.; Nie, S. Alloyed semiconductor quantum dots: Tuning the optical properties without changing the particle size. *J. Am. Chem. Soc.* **2003**, *125* (23), 7100−7106.
(2) Talapin, D. V.; Lee, J.-S.; Kovalenko, M. V.; Shevchenko, E. V. Prospects of colloidal nanocrystals for electronic and optoelectronic applications. *Chem. Rev.* **2010**, *110* (1), 389−458.
(3) Geffroy, B.; le Roy, P.; Prat, C. Organic light-emitting diode (OLED) technology: materials, devices and display technologies. *Polym. Int.* **2006**, *55* (6), 572−582.
(4) Facchetti, A. Semiconductors for organic transistors. *Mater. Today* **2007**, *10* (3), 28−37.
(5) Schöll, A.; Schreiber, F. Molecular Beam Epitaxy. In *From Research to Mass Production* [Online]; Henini, M., Ed.; Elsevier: Amsterdam, 2013; pp 591−609.
(6) Coropceanu, V.; Cornil, J.; da Silva Filho, D. A.; Olivier, Y.; Silbey, R.; Bredas, J.-L. Charge Transport in Organic Semiconductors. *Chem. Rev.* **2007**, *107*, 926−952.
(7) Würthner, F. Bay-substituted perylene bisimides: Twisted fluorophores for supramolecular chemistry. *Pure Appl. Chem.* **2006**, *78* (12), 2341−2349.
(8) Shim, M.; Wang, C.; Norris, D. J.; Guyot-Sionnest, P. Doping and Charging in Colloidal Semiconductor Nanocrystals. *MRS Bull.* **2001**, *26* (12), 1005−1008.
(9) Schimpf, A. M.; Knowles, K. E.; Carroll, G. M.; Gamelin, D. R. Electronic doping and redox-potential tuning in colloidal semiconductor nanocrystals. *Acc. Chem. Res.* **2015**, *48* (7), 1929−37.
(10) Salzmann, I.; Heimel, G.; Oehzelt, M.; Winkler, S.; Koch, N. Molecular Electrical Doping of Organic Semiconductors: Fundamental Mechanisms and Emerging Dopant Design Rules. *Acc. Chem. Res.* **2016**, *49* (3), 370−8.
(11) Boehme, S. C.; Wang, H.; Siebbeles, L. D. A.; Vanmaekelbergh, D.; Houtepen, A. J. Electrochemical charging of CdSe quantum dot films: Dependence on voids size and counterion proximity. *ACS Nano* **2013**, *7* (3), 2500−2508.
(12) Boehme, S. C.; Vanmaekelbergh, D.; Evers, W. H.; Siebbeles, L. D. A.; Houtepen, A. J. In Situ Spectroelectrochemical Determination of Energy Levels and Energy Level Offsets in Quantum-Dot Heterojunctions. *J. Phys. Chem. C* **2016**, *120* (9), 5164−5173.
(13) Bard, A. J.; Faulkner, L. R. *Electrochemical Methods. Fundamentals and Applications*, 2nd ed.; John Wiley & Sons, Inc.: New York, 2001.
(14) Guyot-Sionnest, P. Charging colloidal quantum dots by electrochemistry. *Microchim. Acta* **2008**, *160* (3), 309−314.
(15) Vanmaekelbergh, D.; Houtepen, A. J.; Kelly, J. J. Electrochemical gating: A method to tune and monitor the (opto)electronic properties of functional materials. *Electrochim. Acta* **2007**, *53* (3), 1140−1149.
(16) Hulea, I. N.; Brom, H. B.; Houtepen, A. J.; Vanmaekelbergh, D.; Kelly, J. J.; Meulenkamp, E. A. Wide energy-window view on the density of states and hole mobility in poly(p-phenylene vinylene). *Phys. Rev. Lett.* **2004**, *93* (16), 166601.
(17) Gudjonsdottir, S.; van der Stam, W.; Kirkwood, N.; Evers, W. H.; Houtepen, A. J. The Role of Dopant Ions on Charge Injection and Transport in Electrochemically Doped Quantum Dot Films. *J. Am. Chem. Soc.* **2018**, *140* (21), 6582−6590.
(18) van der Stam, W.; Gudjonsdottir, S.; Evers, W. H.; Houtepen, A. J. Switching between Plasmonic and Fluorescent Copper Sulfide Nanocrystals. *J. Am. Chem. Soc.* **2017**, *139* (37), 13208−13217.
(19) Shimotani, H.; Diguet, G.; Iwasa, Y. Direct comparison of field-effect and electrochemical doping in regioregular poly(3-hexylthiophene). *Appl. Phys. Lett.* **2005**, *86* (2), 022104.
(20) Echegoyen, L.; Echegoyen, L. E. Electrochemistry of Fullerenes and Their Derivatives. *Acc. Chem. Res.* **1998**, *31*, 593−601.
(21) Pei, Q.; Yu, G.; Zhang, C.; Yang, Y.; Heeger, A. J. Polymer Light-Emitting Electrochemical Cells. *Science* **1995**, *269*, 1086−1088.
(22) Gao, J.; Yu, G.; Heeger, A. J. Polymer light-emitting electrochemical cells with frozen p-i-n junction. *Appl. Phys. Lett.* **1997**, *71* (10), 1293−1295.
(23) Matyba, P.; Maturova, K.; Kemerink, M.; Robinson, N. D.; Edman, L. The dynamic organic p−n junction. *Nat. Mater.* **2009**, *8* (8), 672−6.
(24) Tang, S.; Edman, L. Light-Emitting Electrochemical Cells: A Review on Recent Progress. In *Photoluminescent Materials and Electroluminescent Devices*; Armaroli, N., Bolink, H., Eds.; Springer: Cham, 2017.
(25) Pei, Q.; Yang, Y.; Yu, G.; Zhang, C.; Heeger, A. J. Polymer Light-Emitting Electrochemical Cells: In Situ Formation of a Light-Emitting p-n Junction. *J. Am. Chem. Soc.* **1996**, *118* (16), 3922−9.
(26) Tang, S.; Irgum, K.; Edman, L. Chemical stabilization of doping in conjugated polymers. *Org. Electron.* **2010**, *11* (6), 1079−1087.
(27) Wantz, G.; Gautier, B.; Dumur, F.; Phan, T. N. T.; Gigmes, D.; Hirsch, L.; Gao, J. Towards frozen organic PN junctions at room temperature using high-Tg polymeric electrolytes. *Org. Electron.* **2012**, *13* (10), 1859−1864.
(28) Hoven, C. V.; Wang, H.; Elbing, M.; Garner, L.; Winkelhaus, D.; Bazan, G. C. Chemically fixed p−n heterojunctions for polymer electronics by means of covalent B−F bond formation. *Nat. Mater.* **2010**, *9*, 249−252.
(29) Yu, D.; Wang, C.; Wehrenberg, B. L.; Guyot-Sionnest, P. Variable range hopping conduction in semiconductor nanocrystal solids. *Phys. Rev. Lett.* **2004**, *92* (21), 216802.
(30) Houtepen, A. J.; Kockmann, D.; Vanmaekelbergh, D. Reappraisal of Variable-Range Hopping in Quantum-Dot Solids. *Nano Lett.* **2008**, *8* (10), 3516−3520.
(31) Houtepen, A. J. *Charge Injection and Transport in Quantum Confined and Disordered Systems*; Utrecht University: 2007.
(32) Wehrenberg, B. L.; Yu, D.; Ma, J.; Guyot-Sionnest, P. Conduction in Charged PbSe Nanocrystal Films. *J. Phys. Chem. B* **2005**, *109*, 20192−20199.
(33) Qu, L.; Peng, Z. A.; Peng, X. Alternative Routes toward High Quality CdSe Nanocrystals. *Nano Lett.* **2001**, *1* (6), 333−337.
(34) Chen, O.; Zhao, J.; Chauhan, V. P.; Cui, J.; Wong, C.; Harris, D. K.; Wei, H.; Han, H. S.; Fukumura, D.; Jain, R. K.; Bawendi, M. G. Compact high-quality CdSe-CdS core-shell nanocrystals with narrow emission linewidths and suppressed blinking. *Nat. Mater.* **2013**, *12* (5), 445−51.
(35) Hutter, E. M.; Hofman, J.-J.; Petrus, M. L.; Moes, M.; Abellón, R. D.; Docampo, P.; Savenije, T. J. Charge Transfer from Methylammonium Lead Iodide Perovskite to Organic Transport Materials: Efficiencies, Transfer Rates, and Interfacial Recombination. *Adv. Energy Mater.* **2017**, *7* (13), 1602349.
(36) Aulin, Y. V.; Felter, K. M.; Genbas, D. D.; Dubey, R. K.; Jager, W. F.; Grozema, F. C. Morphology-Independent Efficient Singlet Exciton Fissionin Perylene Diimide Thin Films. *ChemPlusChem* **2018**, *83* (4), 230−238.
(37) Ruch, P. W.; Cericola, D.; Hahn, M.; Kötz, R.; Wokaun, A. On the use of activated carbon as a quasi-reference electrode in non-aqueous electrolyte solutions. *J. Electroanal. Chem.* **2009**, *636* (1−2), 128−131.
(38) Noviandri, I.; Brown, K. N.; Fleming, D. S.; Gulyas, P. T.; Lay, P. A.; Masters, A. F.; Phillips, L. The Decamethylferrocenium:Decamethylferrocene Redox Couple- A Superior Redox Standard to the Ferrocenium:Ferrocene Redox Couple for Studying Solvent Effects

DOI: 10.1021/acsanm.9b00863
ACS Appl. Nano Mater. 2019, 2, 4900−4909

on the Thermodynamics of Electron Transfer. *J. Phys. Chem. B* **1999**, *103*, 6713−6722.
(39) Shim, M.; Guyot-Sionnest, P. n-type colloidal semiconductor nanocrystals. *Nature* **2000**, *407*, 981−983.
(40) Hoyer, P.; Weller, H. Potential-Dependent Electron Injection in Nanoporous Colloidal ZnO Films. *J. Phys. Chem.* **1995**, *99* (38), 14096−14100.
(41) Boehme, S. C.; Azpiroz, J. M.; Aulin, Y. V.; Grozema, F. C.; Vanmaekelbergh, D.; Siebbeles, L. D.; Infante, I.; Houtepen, A. J. Density of Trap States and Auger-mediated Electron Trapping in CdTe Quantum-Dot Solids. *Nano Lett.* **2015**, *15* (5), 3056−66.
(42) Murphy, A. R.; Frechet, J. M. J. Organic Semiconducting Oligomers for Use in Thin Film Transistors. *Chem. Rev.* **2007**, *107*, 1066−1096.
(43) Tsumura, A.; Koezuka, H.; Ando, T. Macromolecular electronic device: Field-effect transistor with a polythiophene thin film. *Appl. Phys. Lett.* **1986**, *49* (18), 1210−1212.
(44) Jehoulet, C.; Bard, A. J.; Wudl, F. Electrochemical Reduction and Oxidation of C60 Films. *J. Am. Chem. Soc.* **1991**, *113*, 5456−5457.
(45) Flagg, L. Q.; Giridharagopal, R.; Guo, J.; Ginger, D. S. Anion-Dependent Doping and Charge Transport in Organic Electrochemical Transistors. *Chem. Mater.* **2018**, *30* (15), 5380−5389.
(46) Niu, J.; Conway, B. E.; Pell, W. G. Comparative studies of self-discharge by potential decay and float-current measurements at C double-layer capacitor and battery electrodes. *J. Power Sources* **2004**, *135* (1−2), 332−343.
(47) Zhao, J.; Holmes, M. A.; Osterloh, F. E. Quantum Confinement Controls Photocatalysis- A Free Energy Analysis for Photocatalytic Proton Reduction at CdSe Nanocrystals. *ACS Nano* **2013**, *7* (5), 4316−4325.
(48) Tsui, E. Y.; Hartstein, K. H.; Gamelin, D. R. Selenium Redox Reactivity on Colloidal CdSe Quantum Dot Surfaces. *J. Am. Chem. Soc.* **2016**, *138* (35), 11105−8.
(49) Tsui, E. Y.; Carroll, G. M.; Miller, B.; Marchioro, A.; Gamelin, D. R. Extremely Slow Spontaneous Electron Trapping in Photodoped n-Type CdSe Nanocrystals. *Chem. Mater.* **2017**, *29* (8), 3754−3762.
(50) du Fossé, I.; ten Brinck, S.; Infante, I.; Houtepen, A. J. Role of Surface Reduction in the Formation of Traps in n-Doped II−VI Semiconductor Nanocrystals: How to Charge without Reducing the Surface. *Chem. Mater.* **2019**, *31*, 4575.
(51) Wehrenberg, B. L.; Yu, D.; Ma, J.; Guyot-Sionnest, P. Conduction in Charged PbSe nanocrystal films. *J. Phys. Chem. B* **2005**, *109*, 20192.
(52) Verma, P.; Maire, P.; Novák, P. A review of the features and analyses of the solid electrolyte interphase in Li-ion batteries. *Electrochim. Acta* **2010**, *55* (22), 6332−6341.
(53) Xu, K. Nonaqueous Liquid Electrolytes for Lithium-Based Rechargeable Batteries. *Chem. Rev.* **2004**, *104*, 4303−4417.
(54) Chen, R.; Liu, F.; Chen, Y.; Ye, Y.; Huang, Y.; Wu, F.; Li, L. An investigation of functionalized electrolyte using succinonitrile additive for high voltage lithium-ion batteries. *J. Power Sources* **2016**, *306*, 70−77.
(55) Kim, J. G.; Son, B.; Mukherjee, S.; Schuppert, N.; Bates, A.; Kwon, O.; Choi, M. J.; Chung, H. Y.; Park, S. A review of lithium and non-lithium based solid state batteries. *J. Power Sources* **2015**, *282*, 299−322.
(56) Törmälä, P. Determination of glass transition temperature of poly(ethylene glycol) by spin probe technique. *Eur. Polym. J.* **1974**, *10* (6), 519−521.

DOI: 10.1021/acsanm.9b00863
ACS Appl. Nano Mater. 2019, 2, 4900−4909